

Software tool prototype

Horizon 2020, Grant Agreement no. 869192

Number of the Deliverable
4.4

Due date
31.05.2022

Actual submission date
31.05.2022

Work Package (WP): 4 – Costs and risks assessment

Task: 4.4 – Develop MILP tool

Lead beneficiary for this deliverable: ICL

Editors/Authors: Solene Chiquier, Nixon Sunny, Niall Mac Dowell

Dissemination level: Public

Call identifier: H2020-LC-CLA-02-2019 - Negative emissions and land-use based mitigation assessment

Document history

V	Date	Beneficiary	Authors/ Reviewers
1.0	17.05.2022	ICL	Solene Chiquier (ICL), Nixon Sunny (ICL), Niall Mac Dowell (ICL)/ Lassi Similä (VTT), Antti Lehtilä (VTT)
1.1	31.05.2022	ICL	Solene Chiquier (ICL), Nixon Sunny (ICL), Niall Mac Dowell (ICL)

Partners

VTT – VTT Technical Research Centre of Finland Ltd, Finland
PIK - Potsdam Institute for Climate Impact Research, Germany
ICL - Imperial College of Science Technology and Medicine, United Kingdom
UCAM - University of Cambridge, United Kingdom
ETH - Eidgenössische Technische Hochschule Zürich, Switzerland
BELLONA - Bellona Europa, Belgium
ETA - ETA Energia, Trasporti, Agricoltura, Italy
NIVA - Norwegian Institute for Water Research, Norway
RUG - University of Groningen, Netherlands
INSA - Institut National des Sciences Appliquées de Toulouse, France
CMW - Carbon Market Watch, Belgium
UOXF - University of Oxford, United Kingdom
SE - Stockholm Exergi, Sweden
St1 - St1 Oy, Finland
DRAX - Drax Power Limited, United Kingdom
SAPPI - Sappi Netherlands Services, The Netherlands

Statement of Originality

This deliverable contains original unpublished work except where clearly indicated otherwise. Acknowledgement of previously published material and of the work of others has been made through appropriate citation, quotation or both.

Disclaimer of warranties

The sole responsibility for the content of this report lies with the authors. It does not necessarily reflect the opinion of the European Union. Neither the European Commission nor INEA are responsible for any use that may be made of the information contained therein.

Executive Summary

The purpose of this document is to provide a reference guide as documentation for the software prototype developed in task 4.4 of work package (WP) 4 in the NEGEM project. The tool is implemented in General Algebraic Modeling Systems (GAMS), which is not an open-source software, but it easily interfaces with commercial solvers, allowing the institutional partners in the project to access the software. This documentation does not provide a full algebraic model formulation covering parameters and equations for enhancing brevity. A complete version of the model documentation is to be presented alongside the scenarios explored in Deliverable 4.5 to include scenario-specific constraints in addition to the general model formulation. Nonetheless, the key model components, their functionalities, technology description, and constraint formulation, are covered in this documentation on the software prototype.

The core functionality of the tool is to generate member state-specific pathways for the deployment of negative emissions technologies and practices (NETPs) based on targets for carbon dioxide removal (CDR) and geophysical constraints. The prototype offers the capacity to include multiple NETPs with different system dynamics in a general modelling framework to explore different modelling scenarios. The tool provides insights on deployment pathways and their overall performance as measured through key performance indicators (KPIs) related to cost and environmental impacts.

The prototype features NETPs such as afforestation, bioenergy with carbon capture and storage (BECCS), direct air carbon capture and storage (DACCS), and enhanced weathering (EW). The modelling framework is currently undergoing further development to include other NETPs such as biochar and soil carbon sequestration (SCS), with their associated datasets being developed and expanded upon Deliverables 4.1 and 4.2. In particular, these technologies are modularised in the framework to allow multiple key performance indicators to be evaluated. This provides the capability to integrate the inputs and outputs from work package 1 to quantify the environmental performance of the NETPs in a harmonised approach.

The use of the software prototype, together with the techno- and bio-geophysics databases can be used to explore member state-specific CDR deployment under various constraints. This can quantify the collective capability of EU member states to contribute towards the global CDR budget. Moreover, these scenario investigations provide insights into technology and policy barriers that constrain the deployment rate of NETPs. Thus, helping to develop targeted policy around process and technology intensification to mitigate any environmental and economic risks. Deliverable 4.5 will present analysis of a wide range of scenarios based on different member-state specific CDR ambitions and constraints on technology build rates to inform EU policy on the subject.

Table of contents

Executive Summary	3
List of figures	5
1. Introduction.....	6
2. Model Sets.....	7
2.1 Grid cells.....	7
2.2 Ecological zones.....	7
2.3 Land types.....	8
2.4 Biomass and forest types	8
2.5 Multiple time horizons	8
2.6 Performance metrics	9
3. Technology overview.....	9
3.1 Afforestation.....	9
3.2 Bioenergy with CO ₂ capture and storage (BECCS).....	16
3.3 Direct air CO ₂ capture and storage (DACCS).....	19
3.4 Enhanced Weathering (EW)	21
4. Summary of the optimisation model constraints.....	22
5. References.....	25

List of figures

Figure 1: 28 grid cells used in the simulation and optimisation model prototype to represent the geographical region of EU.	7
Figure 2: 19 global ecological zones used to differentiate between the different kinds of environments in the model prototype.....	7
Figure 3: Equations which compute the cumulative total above-ground biomass stock and mean annual above-ground stock.	10
Figure 4: Equations which compute the timelines attached to the individual forest growth phases.	11
Figure 5: A flow diagram which represents the decision points which involve thinning operations across the forest growth phases.....	12
Figure 6: Equations to compute the overall proportion of above- and below-ground biomass stock over time.	13
Figure 7: Equations to compute the overall CO ₂ pool in various components of the biomass stock.	13
Figure 8: Equations to compute the overall energy requirements of forestry operations.....	15
Figure 9: Equations to compute the overall CO ₂ emissions from forestry operations.	15
Figure 10: Economic evaluation of afforestation based on all the sub-model interactions.	16
Figure 11: Schematic of the BECCS supply chain, outlining the interactions between the sub-models used in the model prototype. Adapted from ^{36,37}	17
Figure 12: Equations to compute the direct land use change effects from clearing the land, and indirect land use change effects.....	17
Figure 13: Equations which compute the CO ₂ footprint of the various processes along the BECCS supply chain.	18
Figure 14: Economic evaluation of BECCS based on all the costs incurred along its value chain.	19
Figure 15: Schematic of the DACCS supply chain, outlining the interactions between the sub-models used in the model prototype.	19
Figure 16: Economic evaluation of DACCS based on all the costs incurred along its value chain.	20
Figure 17: Schematic of the EW supply chain, outlining the interactions between the sub-models used in the model prototype.....	21
Figure 18: Equations which compute the CO ₂ footprint of the various processes along the EW supply chain....	22
Figure 19: Equality and inequality constraints in the optimisation formulation to provide bounds for the key decision variable – the amount of each CDR technology to deploy to meet the cumulative CDR target across member states in the EU.	24

1. Introduction

The aim of this document is to provide a reference guide for the tools and software developed in this project. This section contains a detailed overview of the interaction between a user and the prototype release in GAMS along with the methodology for tailoring the models for application to any specific case study. In GAMS, models are constructed in an abstract manner where the model data is separated from the model to enhance reusability of the model equations without the need for extensive modification with each useⁱ. This style was adopted for the development of the software tool in this project to reduce the development time associated with investigating multiple scenarios.

The GAMS modelling environment consists of four key model entities: Sets, Parameters, Variables and Equations. Sets typically contain a list of items. Parameters contain known values of metrics that are often indexed by components in the sets. Variables are used to describe often unknown/ varying entities in the physical systems during a simulation or optimisation. Equations are used to describe both equality and inequality constraints that apply to the system being studied. The equality constraints (model equations) are strictly enforced and usually do not vary across different scenarios as they represent fundamental relations governing physical flows in the system. But a user may interact with inequality constraints in the model more often than the equality constraints when studying multiple scenarios and optimising the system. For example, if the objective function of an optimisation of the software tool prototype is to minimise the costs of CDR deployment, the model solver would aim to find the least cost solution that satisfies all the optimisation constraints. Here, examples of inequality constraints in the model include EU member state-specific CDR targets (i.e., the amount of CDR deployment by a member state must exceed its national targets). These targets may vary from one scenario to another depending on the total global CDR quota met by the EU, and how they are shared locally.

All users of the model prototype are expected to be able to interact with the modelling environment directly to run multiple scenarios. This document is targeted at both “developers” and “users” alike to benchmark and record the key model components. The document is not intended to be a comprehensive reference of the entire model as the final version of the tool will evolve over the course of the NEGEM project, by incorporating feedback from additional scenario analysis and development, especially within task 4.5.

ⁱ For more information on GAMS, refer to the following documentation: <https://www.gams.com/latest/docs/>

2. Model Sets

2.1 Grid cells

The spatial representation uses a mathematical set in which the elements represent all the potential locations in the overarching spatial region of interest. Ultimately, the number of grid cells in the region is a function of the granularity of dataset and the desired level of spatial aggregation to characterise regional variations in key modelling parameters. For example, the level of precipitation and the general climate depends on the location, and a coarse aggregation of space may overlook the regional differences in the climate and may generate inaccurate estimates of biomass growth.

AT	Austria	IT	Italy
BE	Belgium	LV	Latvia
BG	Bulgaria	LT	Lithuania
HR	Croatia	LU	Luxembourg
CY	Cyprus	MT	Malta
CZ	Czech Republic	NL	Netherlands
DK	Denmark	PL	Poland
EE	Estonia	PT	Portugal
FI	Finland	RO	Romania
FR	France	SK	Slovakia
DE	Germany	SI	Slovenia
EL	Greece	ES	Spain
HU	Hungary	SE	Sweden
IE	Ireland	UK	United Kingdom

Figure 1: 28 grid cells used in the simulation and optimisation model prototype to represent the geographical region of EU.

The model prototype uses a set of 28 cells (see Figure 1) with each cell representing a member-state in the EU (in addition to the UK). The cells follow the natural boundaries separating each country from another, and the overall variations in different model parameters are aggregated at a country-level. In general, open-source Geographical Information Systems (GIS) tools such as QGIS can render highly granular datasets and aggregate them according to approximate polygons covering a country's borders. These GIS tools can be readily interfaced with the model prototype to improve the efficiency of data transfer and eliminate human errors.

2.2 Ecological zones

A mathematical set is used to differentiate between the different ecological zones used in the model. Geophysical datasets are classified according to the ecological zone, containing data on changes in forests, and present states. The global ecological zone map includes tropics, temperate and boreal forests.

P	Polar	SBSk	Subtropical desert
Ba	Boreal coniferous forest	SCs	Subtropical humid forest
Bb	Boreal tundra woodland	SCf	Subtropical dry forest
BM	Boreal mountain systems	SM	Subtropical mountain systems
TeBSk	Temperate steppe	Tar	Tropical rainforest
TeBWk	Temperate desert	Tawa	Tropical moist deciduous forest
TeDc	Temperate continental forest	Tawb	Tropical dry forest
TeDo	Temperate oceanic forest	TBSh	Tropical shrubland
TeM	Temperate mountain systems	TBWh	Tropical desert
SBSk	Subtropical steppe	TM	Tropical mountain systems

Figure 2: 19 global ecological zones used to differentiate between the different kinds of environments in the model prototype.

A total of 20 global ecological zones (see Figure 2) have been defined and mapped according to the Food and Agriculture Organization of the United Nations (FAO)ⁱⁱ, ranging from the evergreen tropical rainforest zone to the boreal tundra woodland zone. A main principle of delineating the global ecological zones involved the aggregation or matching of available regional ecological or potential vegetation maps into the global framework. Many attributes (e.g., land availability) within a systems assessment framework for negative emissions deployment are dependent on the ecological zones.

The type of climate is another mathematical set which differentiates the datasets on temperature, precipitation, etc. The model prototype contains five different climate types as follows: tropical, subtropical, boreal, temperate, and polar.

2.3 Land types

Mathematical sets are used to differentiate between the different types of land which can be used for various purposes. This characterisation helps to screen regions on their capacity to deliver BECCS, EW, and other CDR technologies. Each country has a different proportion of these land types, and this captures geophysical constraints which determine the technical potential of certain types of CDR development in these regions. The set elements are classified as follows: cropland, grassland, forests, marginal agricultural land, land with reforestation potential, and land with harvested wheat.

2.4 Biomass and forest types

The model prototype considers a mathematical set to denote the different biomass and forestry types as they have different features. The crop yield for different species varies, along with their energy content and these factors, amongst others must be incorporated in the modelling framework to improve the accuracy of the deployment estimates. The biomass set elements are as follows: miscanthus, switchgrass, wheat straw, willow, forestry residues. Similarly, the forest types are characterised as either broadleaves or conifers.

Note that these resource types can be imported, stored, and converted in the different regions. These default resource sets can be expanded with additional resources to consider a wider variety of biomass types, with their associated techno-economic parameters.

2.5 Multiple time horizons

All the temporal parameters within the model operate with a base unit. This unit must be consistent across all the different operations in the value chain for the model to be systematic and avoid any inconsistencies. The base unit of time in the model is hours for calculations. A discrete representation of the time horizon accounting for the operating window is combined with a separate, distinct investment time horizon in the model prototype.

The base unit for the investment horizon is a decade, thus investment decisions are taken once every 10-years in the model. The minor time period is used to describe the operational decisions, such as time-dependent production, flow, storage rates, etc. The choice of the minor time periods is dependent on the granularity required by the system. In the model prototype, the core function of the model is to evaluate the overall CDR deployment potential, and there are no granular constraints on an hourly or daily basis. An appropriate

ⁱⁱ FAO global ecological zones: <https://www.fao.org/forest-resources-assessment/remote-sensing/global-ecological-zones-gez-mapping/en/>

aggregation of operational data may use months or seasons to match the granularity observed in the data on precipitation levels, wind speeds, etc. Thus, the set of minor time periods has twelve elements with each corresponding to a month in the year.

2.6 Performance metrics

The set of all performance metrics contain various metrics that are used to evaluate the performance of a given CDR pathway. These metrics may be used to compute the objective function or as part of the model constraints. For example, a set of performance metrics may contain capital expenditure, operating expenditure, together with other metrics such as primary energy consumption, and land use. These metrics may also be relevant for multi-objective optimisation problems when considering the development of NETPs with minimal impacts across a range of KPIs. In particular, this enables the model to evaluate environmental impacts, by integrating the life cycle assessments from work package 1. The model prototype computes KPIs such as land use footprint, water use footprint, primary energy consumption, and the total cost of CO₂ removal.

3. Technology overview

This section presents an overview of the different NETPs covered in the model prototype along with their sub-models and parameters.

3.1 Afforestation

Afforestation is modelled as a series of interactions between the following sub-models: forest growth, forest management, biogenic CO₂ sequestration, fire-risk model, and the forestry operations model.

Within the forest growth model, forest growth rates are characterised by ecological zone, and forest type, to account for a range of geophysical variations. Both the above-ground biomass (the vegetation above the soil, such as stems, branches, foliage, and bark) and the below-ground biomass (i.e., the roots) are included in the forest growth model, as well as dead organic matter.

Within the forest management model, we assume that forest stands are subject to a management approach with minimal human intervention. Forest management maximises the CO₂ sequestration potential of the forest (calculated in the biogenic carbon/ carbon sequestration model) by clearing the forest of old trees, thereby facilitating the growth of the younger trees. This model directly determines the proportion of above-ground biomass that needs to be thinned.

The above-ground biomass stock of reference can be defined as a logistic curve, which is typical in even-aged stands without human intervention. In the model prototype, the above-ground biomass stock of reference, is characterised by ecological zones and parametrised with the IPCC default biomass stock, and net biomass growth rate of natural forests.

```
*/ Reference Curves : Cumulative Above-Ground Biomass Stock & Mean Annual Above-Ground Biomass Stock Curves
```

```
a_CAGBioRef = 99;
T_CAGBioRef(gez) $ AR_Feasible_set(gez) = ceil(BS_AG(gez) / BG_AG(gez));
L_CAGBioRef(gez) $ AR_Feasible_set(gez) = BS_AG(gez);
x0_CAGBioRef(gez) $ AR_Feasible_set(gez) = BS_AG(gez) / (2 * BG_AG(gez));
k_CAGBioRef(gez) $ AR_Feasible_set(gez) = 2 * BG_AG(gez) / BS_AG(gez) * (log(a_CAGBioRef) - log(100 - a_CAGBioRef));

CAGBioRef_ha(gez,yr) $ AR_Feasible_set(gez) = L_CAGBioRef(gez) / (1 + exp(- k_CAGBioRef(gez) * (ord(yr) - x0_CAGBioRef(gez))));
MAAGBioRef_ha(gez,yr) $ AR_Feasible_set(gez) = L_CAGBioRef(gez) / (1+ exp(- k_CAGBioRef(gez) * (ord(yr) - x0_CAGBioRef(gez)))) / ord(yr);
```

Figure 3: Equations which compute the cumulative total above-ground biomass stock and mean annual above-ground stock.

The above-ground biomass stock of reference is calculated for each ecological zone and each year according to the logistic function as captured in Figure 3.

The first 5 equations in Figure 3 compute the following terms:

- The asymptotic coefficient of the reference logistic curve with a default value of 99.
- The growing period of reference in years.
- The maximum biomass stock of reference.
- The mid-point of the reference logistic curve.
- The slope of the reference logistic curve.

Forests may also be managed to maximise wood production for pulp and paper, wood products, bio-energy industries, alongside maintaining their CO₂ sequestration potentials. The afforested above-ground biomass stock can be derived from the above-ground biomass stock of reference, subject to a forest management cycle.

Forest growth is usually characterised by the following five phases — establishment, initial growth, full-vigour, maturity, and old-growth phases (see Figure 4). Forest management accounts for each of these phases to determine the frequency of harvesting/thinning operations, and its intensity. The frequency and intensity of harvesting/thinning operations are specific to each phase and evolve over time.

Forest growth phases are determined based on the Mean Annual Increment (MAI), which is the average rate of merchantable volume of biomass growth, and the Maximum Mean Annual Increment (MMAI). However, in the context of CO₂ removal, both merchantable and non-merchantable biomass stocks must be considered covering both above- and below-ground biomass stocks.

Thus, in this model prototype, we introduce the Mean Annual Growth (MAG), which is defined as the average rate of dry-mass of above-ground biomass growth; and the Maximum Mean Annual Growth (MMAG), which replace the MAI and the MMAI, respectively.

```

*/ Forest Growth Phases : Durations, Ends of Phases & Characteristics

*/ Establishment Phase - Usually 5 years
yr_End_EstablishmentPhase = EstablishmentPhase_User;

*/ Initial Phase - Until First Thinning (Usually 25 years AFTER Establishment Phase) but 10 years in MONET
yr_End_InitialPhase = FirstThinning_User + yr_End_EstablishmentPhase;
Duration_InitialPhase = FirstThinning_User;

*/ Full Vigour Phase - Until Maximum MAI
MMAI(gez) $ AR_Feasible_set(gez) = smax(yr $ (ord(yr) > Duration_InitialPhase), MAAGBioRef_ha(gez,yr));

loop ( (gez,yr), yr_MMAI(gez) $ (MAAGBioRef_ha(gez,yr) = MMAI(gez) AND AR_Feasible_set(gez)) = ord(yr);
);

*/ Mature Phase - Usually Until Half-MMAI
Half_MMAI(gez) $ AR_Feasible_set(gez) = MMAI(gez)/2;

*/ Old-Growth Phase - Usually Until the End of the GHG Accounting but 300 yrs in MONET
yr_End_OldGrowthPhase = card(yr);

```

Figure 4: Equations which compute the timelines attached to the individual forest growth phases.

Figure 4 describes the overarching equations governing each of the five phases of forest growth. A schematic of the forest management approach is described via Figure 5, where:

- $yr_{E,END}$ is the last year of the establishment phase (years) with a default value of 15 years.
- $yr_{I,END}$ is the last year of the initial phase (years), with a default value of 5 years.
- MAG_{BT}^{AG} is the mean annual growth (MAG), before thinning (tonnes_{DM}/ha/yr),
- $MMAG_{Ref}^{AG}$ is the maximum mean annual growth (tonnes_{DM}/ha/yr), AT is the annual thinning stock (tonnes_{DM}/ha),
- $\%_T$ is the thinning share of the above-ground biomass stock (%),
- B_{BT}^{AG} is the above-ground biomass stock, before thinning (tonnes_{DM}/h¹),
- $yr_{last FVT}$ is the year during which the last thinning of the full-vigour phase occurred (years),
- and $yr_{last MT}$ is the year during which the last thinning of the mature phase occurred (years).

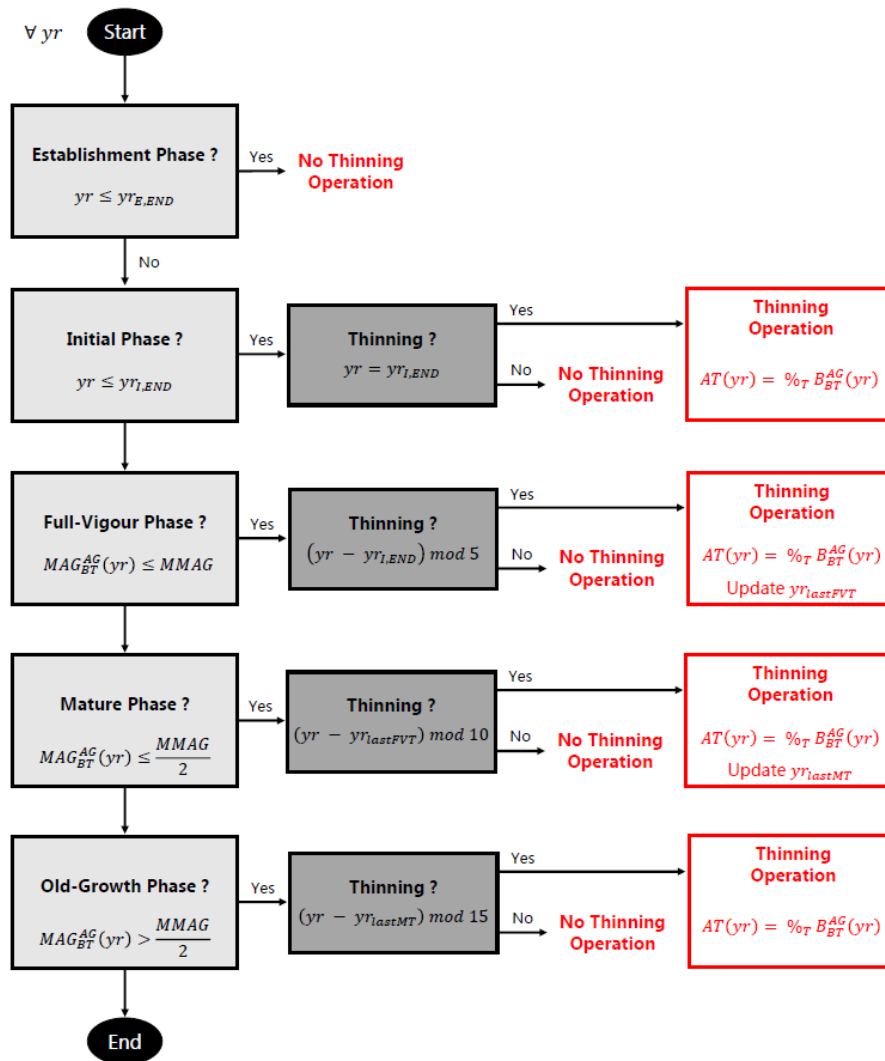


Figure 5: A flow diagram which represents the decision points which involve thinning operations across the forest growth phases.

The below-ground biomass stock is estimated from the above-ground biomass stock using a "root-to-shoot" ratio. This ratio usually depends on the climate, tree species, soil type, and declines with stand age and/or productivity. In the model prototype, the "root-to-shoot" ratio evolves with the amount of above-ground biomass stock as according to data presented by the IPCCⁱⁱⁱ. The total biomass content is computed as the total of both above- and below-ground biomass stocks as shown in Figure 6 below.

ⁱⁱⁱ <https://www.ipcc-nggip.iges.or.jp/public/2006gl/vol4.html>

```

*// Total (Above-Ground & Below-Ground) Biomass

* 1/ Before Thinning
CTotalBio_BT_ha(gez,sp,yr) $ AR_Feasible_set(gez) = CAGBio_BT_ha(gez,yr) + CBGBio_BT_ha(gez,sp,yr);

* 2/ Thinning
ATotalBioLosses_ha(gez,sp,yr) $ AR_Feasible_set(gez) = AThinning_ha(gez,yr) + ABGBioLosses_ha(gez,sp,yr);
CTotalBioLosses_ha(gez,sp,yr) $ AR_Feasible_set(gez) = CThinning_ha(gez,yr) + CBGBioLosses_ha(gez,sp,yr);

* 3/ After Thinning
AAGBio_AT_ha(gez,yr) $(AR_Feasible_set(gez) AND ord(yr) = 1) = CAGBio_AT_ha(gez,yr);
AAGBio_AT_ha(gez,yr) $(AR_Feasible_set(gez) AND ord(yr) > 1) = CAGBio_AT_ha(gez,yr) - CAGBio_AT_ha(gez,yr-1);

CTotalBio_AT_ha(gez,sp,yr) $ AR_Feasible_set(gez) = CAGBio_AT_ha(gez,yr) + CBGBio_AT_ha(gez,sp,yr);

ATotalBio_AT_ha(gez,sp,yr) $(AR_Feasible_set(gez) AND ord(yr) = 1) = CTotalBio_AT_ha(gez,sp,yr);
ATotalBio_AT_ha(gez,sp,yr) $(AR_Feasible_set(gez) AND ord(yr) > 1) = CTotalBio_AT_ha(gez,sp,yr) - CTotalBio_AT_ha(gez,sp,yr-1);

```

Figure 6: Equations to compute the overall proportion of above- and below-ground biomass stock over time.

Growing forests capture CO₂ from the atmosphere via photosynthesis. The CO₂ is sequestered in the form of carbon to the above-ground biomass, which is then partially transferred to the below-ground biomass, dead organic matter, and soil. During harvesting or thinning operations, timber and forest residues are extracted from the forest stands and are considered as "harvested wood products".

The above-ground biomass carbon pool is comprised of all carbon that is contained in the vegetation above the soil, such as stems, branches, foliage or bark, and the below-ground biomass carbon pool is comprised of the carbon contained in the roots. Together, they constitute the total biomass carbon pool, of which the carbon stock can be estimated from the biomass stock with the use of a carbon content factor (see Figure 7). This factor depends on climate, forest type, such as conifers or broadleaves, and tree characteristics, such as age, size, or tree parts.

```

*// Total CO2 Stock

*// per HECTARE
ACO2_ha(gez,sp,yr) = ACO2_TotalBio_AT_ha(gez,sp,yr) + Ind_Litter * ACO2_Litter_ha(gez,sp,yr);
CCO2_ha(gez,sp,yr) = CCO2_TotalBio_AT_ha(gez,sp,yr) + Ind_Litter * CCO2_Litter_ha(gez,sp,yr);

*// per ABOVE-GROUND BIOMASS
CCO2_AGBio(gez,sp,yr) = CCO2_TotalBio_AT_AGBio(gez,sp,yr) + Ind_Litter * CCO2_Litter_AGBio(gez,sp,yr);

```

Figure 7: Equations to compute the overall CO₂ pool in various components of the biomass stock.

Overall, within the biogenic carbon sequestration model, the CO₂ sequestration potential of AR has an oscillating S-curve pattern of growth, and it is characterised by ecological zones and forest types.

Afforestation is affected by wildfires, insects, adverse weather events, harvesting, or active deforestation which decreases its CO₂ sequestration potential over time. With continued global warming, the likelihood of adverse events increases, thereby reducing the CO₂ losses along the afforestation value chain. In the model prototype, we model the risk of wildfires using a penalty coefficient to evaluate their impacts on the CO₂ sequestration potential of afforestation.

The model prototype is adapted from a risk-accounting methodology developed in Hurteau et al.¹ to define a wildfire-penalty coefficient, which is characterised by ecological zones, and applicable at the country level. The penalty coefficient is based on the severity of a wildfire (the potential biomass loss given a fire occurrence) and the probability of a fire event occurring during a specified period.

Afforestation requires the establishment and the on-going maintenance of the forest to maximise and maintain CDR. These include site establishment, forest roads construction, maintenance, and thinning operations. The forest is established by land preparation and planting of new seedlings. For land preparation, mounding is carried out by an excavator²⁻⁴, and herbicide and fertiliser are applied using a tractor^{2,4}. Tree seedlings are prepared⁵, then planted by hand^{2,4,6}.

As part of forest management, a selection of trees is thinned using a cut-to-length logging system. This involves the extraction of trees from the forest site using a combination of harvesters and forwarders^{30,32}. Here, we assume that the selection of forest biomass is composed of 80% thinning and 20% forest residues, such as branches, foliage, or bark⁹. Early whole tree thinning involves tree felling by harvesters, followed by whole tree removal from the site to the roadside by forwarders. Harvesting roundwood requires harvesters that cut the trees, leaving branches and other forest residues on the forest floor. Approximately a third of the forestry residues are left on the forest floor to maintain the nutrient and soil carbon balance, and the remainder is collected by forwarders that compress the residues into bundles. All thinned and extracted forest biomass are stored at the roadside for natural drying^{2,9}.

Accordingly, in the model prototype, the following operations are defined: forest establishment, forest road construction, and forest maintenance. These forestry operations are assessed on their energy requirements (see Figure 8) and associated CO₂ and N₂O emissions^{30,32} (see Figure 9). These KPIs are computed based on the following processes:

- the production and combustion of fuels (diesel and petrol)¹⁰ for the establishment and the management of the forest, and for the construction and maintenance of forest roads.
- the manufacture of feedstocks and other materials (herbicide and fertiliser), seedlings¹¹⁻¹³, road rocks and aggregates^{2,3,10}.
- direct and indirect land-use change.

Direct N₂O emissions from the application of nitrogen-based fertiliser during the forest establishment and from the use of ammonium nitrate-based explosive for road rocks extraction are included in the model¹⁴⁻¹⁷. The energy requirements and emission sources are characterised into midpoint and endpoint impact scores in the sustainability assessments presented in work package 1. The primary data used here to inform the model instance aligns with that used in work package 1 to ensure model consistency.

```

1 *****
2 * Parameters Calculations: Energy Model
3 *****
4
5 loop((c,gez) $ AR_RefCases_set(c,gez),
6
7 /*/ Initial Forestry Operations
8 tER_IniFOP_ha(c,e,del) $(ord(del) <= Horizon_delay_card) = sum(time $(ord(time) = ord(del)), ER_GP_ha(e,time) * Ind_GroundPrep + ER_SPrP1_ha(c,e,time) * Ind_Seedlings +
9
10 /*/ Annual Forestry Operations
11
12 * Note : After the Establishment Phase
13 tER_AFOP_ha(c,gez,sp,e,t,del) $(HC_AR_t_set(gez,t,del) AND ord(t) > t_establishment(del,gez) AND ord(t) <= Horizon_time) = sum((yr,time) $(ord(yr) = ord(t) - t0(del) A
14
15 * Note : After the Establishment Phase and After 2100
16 tER_AFOP_ha(c,gez,sp,e,t,del) $(HC_AR_t_set(gez,t,del) AND ord(t) > t_establishment(del,gez) AND ord(t) > Horizon_time) = sum((yr,time) $(ord(yr) = ord(t) - t0(del) AN
17
18 /*/ Annual Energy Requirements
19
20 * Note : During the Establishment Phase
21 AEnergy_t_ha(c,gez,sp,e,t,del) $(HC_AR_t_set(gez,t,del) AND ord(t) <= t_establishment(del,gez) AND yr_End_EstablishmentPhase <> 0) = tER_IniFOP_ha(c,e,del)/yr_End_Esta
22
23 * Note : After the Establishment Phase
24 AEnergy_t_ha(c,gez,sp,e,t,del) $(HC_AR_t_set(gez,t,del) AND ord(t) > t_establishment(del,gez)) = tER_AFOP_ha(c,gez,sp,e,t,del);
25
26 /*/ Cumulative Forestry Operations
27 CEnergy_t_ha(c,gez,sp,e,t,del) $ HC_AR_t_set(gez,t,del) = sum(t_ $(ord(t_) <= ord(t)) , AEnergy_t_ha(c,gez,sp,e,t_,del));
28
29 /*/ Optimisation Annual & Cumulative Energy Requirements
30 * Warning : Calculating AEnergy_d_ha doesn't make sense ...
31 * AEnergy_d_ha(c,gez,sp,e,decade,del) $ HC_AR_d_set(gez,decade,del) = sum(t $(ord(t) = ta(decade)), AEnergy_t_ha(c,gez,sp,e,t,del));
32 CEnergy_d_ha(c,gez,sp,e,decade,del) $ HC_AR_d_set(gez,decade,del) = sum(t $(ord(t) = tc(decade)), CEnergy_t_ha(c,gez,sp,e,t,del));
33 avAEnergy_d_ha(c,gez,sp,e,decade,del) $ HC_AR_d_set(gez,decade,del) = (CEnergy_d_ha(c,gez,sp,e,decade,del) / 10) $(ord(decade) = 1) + ((CEnergy_d_ha(c,gez,sp,e,decade,de
34 ) ;

```

Figure 8: Equations to compute the overall energy requirements of forestry operations.

```

32 /*/ CO2 Emitted
33
34 /*/ Initial Forestry Operations
35
36 * Note : During the Establishment Phase
37 tECO2_IniFOP_ha(c,del) $(ord(del) <= Horizon_delay_card) = sum(time $(ord(time) = ord(del)), CF_GP_ha(time) * Ind_GroundPrep + CF_SPrP1_ha(c,time) * Ind_Seedlings + CF_R
38
39 /*/ Annual Forestry Operations
40
41 * Note : After the Establishment Phase
42 tECO2_AFOP_ha(c,gez,sp,t,del) $(HC_AR_t_set(gez,t,del) AND ord(t) > t_establishment(del,gez) AND ord(t) <= Horizon_time) = sum((yr,time) $(ord(yr) = ord(t) - t0(del) A
43
44 * Note : After the Establishment Phase and After 2100
45 tECO2_AFOP_ha(c,gez,sp,t,del) $(HC_AR_t_set(gez,t,del) AND ord(t) > t_establishment(del,gez) AND ord(t) > Horizon_time) = sum((yr,time) $(ord(yr)=ord(t) - t0(del) AND
46
47 /*/ Annual GHG Emissions
48
49 * Note : During the Establishment Phase
50 AECO2_t_ha(c,gez,sp,t,del) $(HC_AR_t_set(gez,t,del) AND ord(t) <= t_establishment(del,gez) AND yr_End_EstablishmentPhase <> 0) = tECO2_IniFOP_ha(c,del) / yr_End_Establ
51
52 * Note : After the Establishment Phase
53 AECO2_t_ha(c,gez,sp,t,del) $(HC_AR_t_set(gez,t,del) AND ord(t) > t_establishment(del,gez)) = tECO2_AFOP_ha(c,gez,sp,t,del);
54
55 /*/ Cumulative Forestry Operations
56 CEEO2_t_ha(c,gez,sp,t,del) $ HC_AR_t_set(gez,t,del) = sum(t_ $(ord(t_) <= ord(t)), AECO2_t_ha(c,gez,sp,t_,del));

```

Figure 9: Equations to compute the overall CO₂ emissions from forestry operations.

Similarly, the total costs of afforestation are computed using:

- the cost of energy (*i.e.* fuels¹⁸ and electricity^{19–23}) and the amount used.
- the cost of machinery – trucks or excavators for land preparation, harvesters and forwarders for harvesting operations, and other machinery for road construction and maintenance^{24,25}.
- the cost of labour – ground workers, forest workers, road operators²⁶, etc.

- the cost of feedstocks and other materials, *i.e.* agrochemicals^{27,28}, seedlings²⁹, and road rocks³⁰.

The costs, calculated via the equations in Figure 10, are expressed in 2018 US \$ but disaggregated at the national level. Cost datasets from other countries are converted using exchange rates for the currency and US \$ and inflation factors^{31,32}. The costs of afforestation are levelised using a capital recovery factor (CRF), which is computed using the desired interest rate in % and the desired financial lifetime in years.

```

1 *****
2 * Parameters Calculations: Cost Models
3 *****
4
5 loop((c,gez) $ AR_RefCases_set(c,gez),
6
7 /* Financial Parameters
8
9 IR_AR $(IR_AR_User <> 0) = IR_AR_User;
10 IR_AR $(IR_AR_User = 0) = IR_dAR;
11
12 CRF_AR $(IR_AR + 1) = (IR_AR * (IR_AR + 1) **LT_AR) / ((IR_AR + 1)** LT_AR - 1);
13
14
15 /* Initial & Annual Costs
16
17 /* Initial Forestry Operations
18
19 * Note : During the Establishment Phase
20 tCost_IniFop_ha(c,sp,delat) $(ord(delat) <= Horizon_delat_card) = sum(time $(ord(time) = ord(delat)), Cost_GP_ha(c,time) * Ind_GroundPrep + Cost_SPrP1_ha(c,sp,time) * Ind_Seed
21
22 /* Annual Forestry Operations
23
24 * Note : After the Establishment Phase
25 tCost_AFOP_ha(c,gez,sp,t,delat) $(HC_AR_t_set(gez,t,delat) AND ord(t) > t_establishment(delat,gez) AND ord(t) <= Horizon_time) = sum((yr,time) $(ord(yr) = (ord(t) - t0(delat))
26
27 * Note : After the Establishment Phase and After 2100
28 tCost_AFOP_ha(c,gez,sp,t,delat) $(HC_AR_t_set(gez,t,delat) AND ord(t) > t_establishment(delat,gez) AND ord(t) > Horizon_time) = sum((yr,time) $(ord(yr) = (ord(t) - t0(delat))

```

Figure 10: Economic evaluation of afforestation based on all the sub-model interactions.

3.2 Bioenergy with CO₂ capture and storage (BECCS)

This subsection details the modelling of the BECCS supply chain – land use change, biomass cultivation, processing and feedstock transport, biomass to energy conversion with CO₂ capture, CO₂ transport and storage. In the prototype, different types of crops are cultivated and analysed. Owing to the “carbon debt” initiated by land conversion to biomass production (depending on the type of land converted^{33–35}), it usually takes some time for BECCS projects to bring net negative emissions. Accordingly, the CO₂ removal potential of BECCS is calculated over time. A schematic representation of the sub-models used to characterise BECCS is shown in Figure 11.

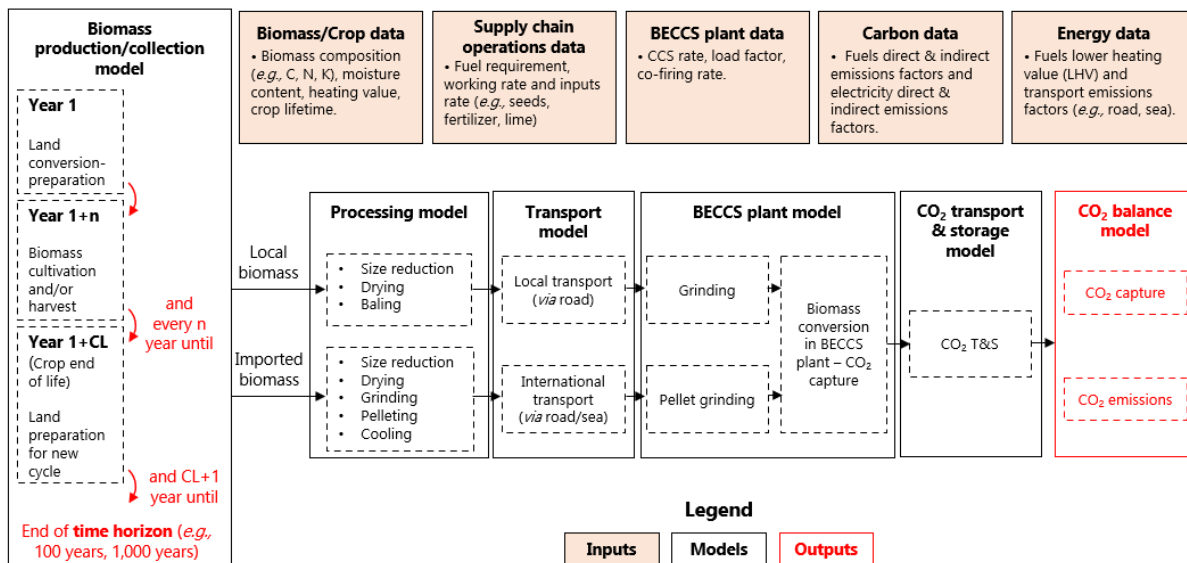


Figure 11: Schematic of the BECCS supply chain, outlining the interactions between the sub-models used in the model prototype. Adapted from ^{36,37}.

Direct land use changes are changes in soil and vegetation carbon stocks between the new and previous uses of the land. Indirect land use changes, on the other hand, are unintended consequence of releasing more CO₂ emissions owing to the additional land use changes around the world, induced by the displacement of agricultural land, such as cropland or grassland, elsewhere to meet demand. The conversion of the land on which the biomass is cultivated for BECCS creates both direct and indirect land use change effects. (I)LUCs are associated with a CO₂ footprint, which needs to be compensated by BECCS’s CO₂ removal potential for the technology to offer value. But this depends on the type of land on which the biomass is grown for BECCS.

For example, converting an existing cropland into biomass cultivation for BECCS, results into 37,500 kgCO₂/ha of LUC³³ (due to the clearing of the land, and therefore the destruction of the natural CO₂ sink), but also 0.2 tCO₂/ha of ILUC^{34,35}, because the activity must be displaced and that will create LUC somewhere else. LUC effects are considered within the model prototype to define the overall value of BECCS considering multiple KPIs (see Figure 12).

```

9   */// Land Use Change
10  CF_LUC_ha(b,1,a) $ (ord(a)=1 AND Ind_FeasibleLand(b,1)) = LUC(1) * (1-Ind_Res(b));
11  CF_ILUC_ha(b,1,a) $ (ord(a)=1 AND Ind_FeasibleLand(b,1)) = ILUC(1) * (1-Ind_Res(b));

```

Figure 12: Equations to compute the direct land use change effects from clearing the land, and indirect land use change effects.

Overall, the CO₂ removal potential of BECCS is the difference between the CO₂ captured initially via photosynthesis during the biomass growth, and the total GHG emissions arising from all steps of the biomass supply chain, the amount of CO₂ captured in the BECCS plant, and the CO₂ emissions incurred along the CO₂ transport and storage chain. Note that the supply chain CO₂ footprint is assumed to evolve over time in an exogenous manner, based on the ongoing decarbonisation of the fuel and electricity supply chains, according to latest projections by organisations such as the International Energy Agency and EU REF 2020 scenarios^{iv}. A user

iv https://energy.ec.europa.eu/data-and-analysis/energy-modelling/eu-reference-scenario-2020_en

may investigate multiple scenarios with different realisations of these exogenous parameters to evaluate the overall CDR potential according to the model assumptions.

The BECCS plant is assumed to generate power in this instance, but this is not a concrete parameter, and a user can vary the techno-economic dataset to reflect the inputs and outputs of alternative BECCS configurations. Nonetheless, the fundamental relations are captured through the equations in Figure 13.

```

106  */ BECCS CO2 Emissions Model
107
108  */ BECCS CO2 Balance
109  CF_ha(sr,sr_,b,l,p,p_,t,a,time) $ Ind_FeasibleOptSCPort(sr,sr_,b,l,p,p_,t) = CF_SC_ha(sr,sr_,b,l,p,p_,t,a,time) + CF_Coal(sr,sr_,b,t,a) + CF_TS_ha(sr,sr_,b,t,a,time);
110  tCF_ha(sr,sr_,b,l,p,p_,t,time) $ Ind_FeasibleOptSCPort(sr,sr_,b,l,p,p_,t) = sum(a $(ord(a) <= PL), CF_ha(sr,sr_,b,l,p,p_,t,a,time));
111  tCF(sr,sr_,b,l,p,p_,t,time) $(Ind_FeasibleOptSCPort(sr,sr_,b,l,p,p_,t) AND tPellet(sr,sr_,b,t)) = tCF_ha(sr,sr_,b,l,p,p_,t,time) / tPellet(sr,sr_,b,t);
112
113  nCF_ha(sr,sr_,b,l,p,p_,t,a,time) $ Ind_FeasibleOptSCPort(sr,sr_,b,l,p,p_,t) = CF_SC_ha(sr,sr_,b,l,p,p_,t,a,time) + nCF_Coal(sr,sr_,b,t,a) + nCF_TS_ha(sr,sr_,b,t,a,time);
114  tnCF_ha(sr,sr_,b,l,p,p_,t,time) $ Ind_FeasibleOptSCPort(sr,sr_,b,l,p,p_,t) = sum(a $(ord(a) <= PL), nCF_ha(sr,sr_,b,l,p,p_,t,a,time));
115  tnCF(sr,sr_,b,l,p,p_,t,time) $(Ind_FeasibleOptSCPort(sr,sr_,b,l,p,p_,t) AND tPellet(sr,sr_,b,t)) = tnCF_ha(sr,sr_,b,l,p,p_,t,time) / tPellet(sr,sr_,b,t);
116
117  RCO2_ha(sr,sr_,b,l,p,p_,t,a,time) $ Ind_FeasibleOptSCPort(sr,sr_,b,l,p,p_,t) = SCO2_ha(sr,sr_,b,t,a) - CF_ha(sr,sr_,b,l,p,p_,t,a,time);
118  tRCO2_ha(sr,sr_,b,l,p,p_,t,a,time) $ Ind_FeasibleOptSCPort(sr,sr_,b,l,p,p_,t) = sum(a $(ord(a)<ord(a)), RCO2_ha(sr,sr_,b,l,p,p_,t,a,time));
119  tRCO2(sr,sr_,b,l,p,p_,t,time) $ Ind_FeasibleOptSCPort(sr,sr_,b,l,p,p_,t) = sum(a $(ord(a) <= PL), RCO2_ha(sr,sr_,b,l,p,p_,t,a,time));
120  tRCO2(sr,sr_,b,l,p,p_,t,time) $(Ind_FeasibleOptSCPort(sr,sr_,b,l,p,p_,t) AND tPellet(sr,sr_,b,t)) = tRCO2_ha(sr,sr_,b,l,p,p_,t,time) / tPellet(sr,sr_,b,t);
121
122  Ind_AnnualNegScenarios(sr,sr_,b,l,p,p_,t,a,time) $(CRCO2_ha(sr,sr_,b,l,p,p_,t,a,time) <= 0 AND Ind_FeasibleOptSCPort(sr,sr_,b,l,p,p_,t) = 1;
123  CBET(sr,sr_,b,l,p,p_,t,time) $(Ind_FeasibleOptSCPort(sr,sr_,b,l,p,p_,t) AND tRCO2(sr,sr_,b,l,p,p_,t,time) > 0) = sum (a, Ind_AnnualNegScenarios(sr,sr_,b,l,p,p_,t,a,time))

```

Figure 13: Equations which compute the CO₂ footprint of the various processes along the BECCS supply chain.

The total cost of the BECCS system is likely to be greatly influenced by CAPEX, biomass cultivation and harvest costs, processing, and transport costs. It is important to study the effect of the biomass supply chain configuration on the total cost of BECCS within each region. Some feedstocks such as agricultural and forestry residues are likely to be available at lower costs depending on the region, and this may generate an economic merit order for the plant input. The total system costs are also likely to be influenced by variations in fuel and electricity prices, biomass yields, and energy systems.

The total cost of BECCS deployment is characterised by the following components in the model:

- the cost of energy for biomass cultivation, harvest, processing and transport, biomass processing, and CO₂ transport and storage.
- the CAPEX and OPEX of BECCS plants³⁸, together with the associated infrastructure costs.
- the cost of machinery for biomass cultivation, harvest and processing, and biomass transport.
- the cost of labour – farmers, BECCS plant operators, truck drivers.
- the cost of feedstocks, materials, agrochemicals (fertilizers, herbicides, and lime).
- the cost of land.

The CAPEX of the BECCS plant is levelised using a CRF, which is computed using the same assumptions as for afforestation. Moreover, a learning rate-based cost reduction of 30% is assumed between 2020 and 2050 for CAPEX, in line with the IEA estimates³⁸. The sale of the electricity produced at the BECCS plant provides revenues, which are assumed to be priced at the sub-regional wholesale value of electricity as reported in Deliverable 4.2. There is uncertainty around the average wholesale market price of electricity in the future with increasing penetration of renewables and a diversified electricity generation mix. Current estimates of electricity prices may be unsuitable for estimating revenue shares, and this will need to be explored through multiple scenarios to provide contrasting findings and build confidence. Overall, the net cost of BECCS is the total costs of BECCS less the revenue from the production of electricity at the BECCS plant. Figure 14 presents the governing equations for the economic evaluation of BECCS.

```

236 */ BECCS Total Cost & Cost Balance
237 Cost_ha(sr,sr_,b,l,p,p_,t,a,time) $ Ind_FeasibleOptSCPort(sr,sr_,b,l,p,p_,t) = Cost_SC_ha(sr,sr_,b,l,p,p_,t,a,time) + Cost_PP_ha(sr,sr_,b,t,a,time) + Cost_CO2TS_ha(sr,
238
239 tCost_ha(sr,sr_,b,l,p,p_,t,time) $ Ind_FeasibleOptSCPort(sr,sr_,b,l,p,p_,t) = sum(a $ (ord(a) <= PL), Cost_ha(sr,sr_,b,l,p,p_,t,a,time));
240 tcost(sr,sr_,b,l,p,p_,t,time) $(Ind_FeasibleOptSCPort(sr,sr_,b,l,p,p_,t) AND tPellet(sr,sr_,b,t)) = tCost_ha(sr,sr_,b,l,p,p_,t,time) / tPellet(sr,sr_,b,t);
241 tCost_SCO2(sr,sr_,b,l,p,p_,t,time) $(Ind_FeasibleOptSCPort(sr,sr_,b,l,p,p_,t) AND tSCO2_ha(sr,sr_,b,t))= tCost_ha(sr,sr_,b,l,p,p_,t,time)/(tSCO2_ha(sr,sr_,b,t)/1000);
242 tCost_MWh(sr,sr_,b,l,p,p_,t,time) $(Ind_FeasibleOptSCPort(sr,sr_,b,l,p,p_,t) AND tEG_P_ha(sr,sr_,b,t))= tCost_ha(sr,sr_,b,l,p,p_,t,time)/(tEG_P_ha(sr,sr_,b,t)/3600);
243
244
245 BE_NEC(sr,sr_,b,l,p,p_,t,time) $(Ind_FeasibleOptTPort(sr,sr_,b,p,p_,t) AND Ind_NegScenario(sr,sr_,b,l,p,p_,t,time) AND tRCO2(sr,sr_,b,l,p,p_,t,time)) = (tcost(sr,sr_,
246
247 tCB_ha(sr,sr_,b,l,p,p_,t,time) $ Ind_FeasibleOptSCPort(sr,sr_,b,l,p,p_,t) = tCost_ha(sr,sr_,b,l,p,p_,t,time) - trev_PP(sr,sr_,b,l,p,p_,t,time) * tPellet(sr,sr_,b,t);
248 tCB(sr,sr_,b,l,p,p_,t,time) $ Ind_FeasibleOptSCPort(sr,sr_,b,l,p,p_,t) = tcost(sr,sr_,b,l,p,p_,t,time) - trev_PP(sr,sr_,b,l,p,p_,t,time);
249 tCB_SCO2(sr,sr_,b,l,p,p_,t,time) $(Ind_FeasibleOptSCPort(sr,sr_,b,l,p,p_,t) AND tSCO2_ha(sr,sr_,b,t)) = tCB_ha(sr,sr_,b,l,p,p_,t,time)/(tSCO2_ha(sr,sr_,b,t)/1000);
250 tCB_MWh(sr,sr_,b,l,p,p_,t,time) $(Ind_FeasibleOptSCPort(sr,sr_,b,l,p,p_,t) AND tEG_P_ha(sr,sr_,b,t)) = tCB_ha(sr,sr_,b,l,p,p_,t,time)/(tEG_P_ha(sr,sr_,b,t)/3600);

```

Figure 14: Economic evaluation of BECCS based on all the costs incurred along its value chain.

3.3 Direct air CO₂ capture and storage (DACCS)

Two process configurations are modelled for DACCS – a solid sorbent- and a liquid solvent-based capture of CO₂ from the air³⁹. For the liquid solvent DACCS, high-grade heat is assumed to be provided by natural gas, hydrogen, or electricity in the different process archetypes. Based on (Keith et al., 2018)⁴⁰, the CO₂ emissions generated from the combustion of natural gas are captured by the CCS unit. For the solid sorbent DACCS, both heat and power are provided by the electricity grid, and we assume that a heat pump, with a coefficient of performance of 3, is used to convert grid power to low-grade heat. This DACCS value chain is captured in Figure 15.

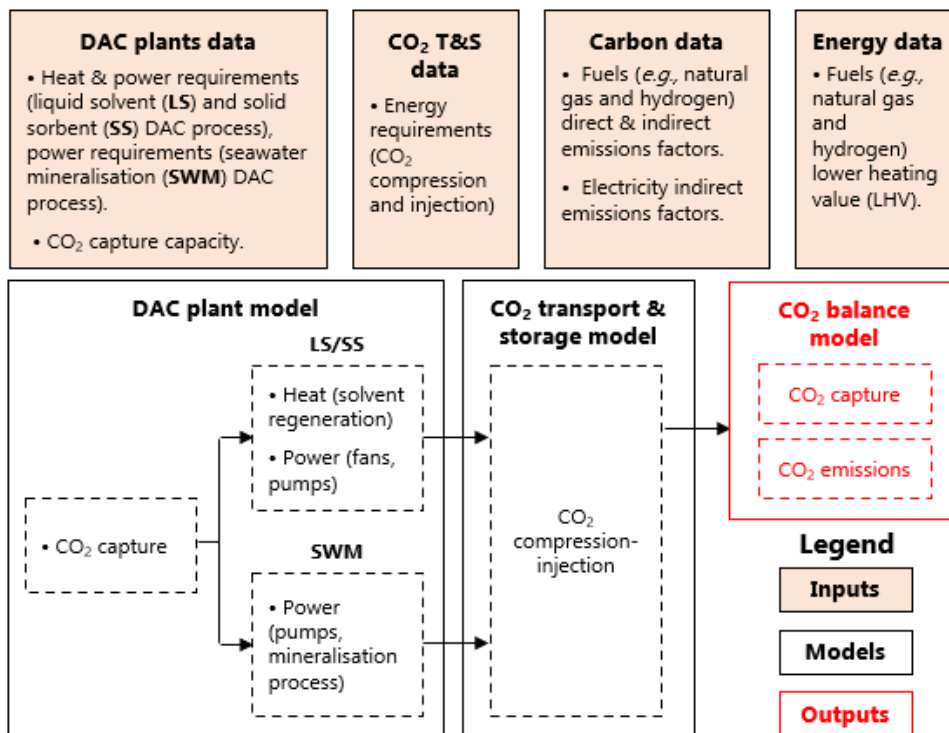


Figure 15: Schematic of the DACCS supply chain, outlining the interactions between the sub-models used in the model prototype.

The effective CO₂ removal potential of DACCS is a function of the carbon intensity of the energy used, which varies with region and time. In the model prototype, the total GHG emissions of DACCS include:

- direct CO₂ emissions from the combustion of natural gas in the DACCS system as a function of the CO₂ capture rate.
- indirect CO₂ emissions from the supply of natural gas, hydrogen, or power to support the DACCS plant.

The total costs of DACCS are evaluated by combining:

- the CAPEX and OPEX of the DAC plant, CO₂ transport and storage, including labour, operating and maintenance costs^{40,41}.
- the cost of energy supply needed to provide the heat^{19,22,42–44} and power^{19–23}.

The total cost of liquid solvent DACCS archetype is based on a process design published by Carbon Engineering⁴⁰ and from a report from the National Academies of Sciences, Engineering, and Medicine³⁹. In Keith *et al.*⁴⁰, the total levelised cost of CO₂ capture of DACCS is estimated as \$113–168/t CO₂ captured. As these estimates are aligned with the lower bound of DACCS total cost range reported in the literature^{45,46} (\$25–1,000/t CO₂), we assume that the total cost of DACCS (including CAPEX, OPEX, and energy) is approximately \$400–600/t CO₂ captured, both using a reference year of 2018.

```

234  *// DAC Plant Cost
235
236  */// Financial Parameters
237  LT_DP = LT_DP_User $(LT_DP_User <> 0) + LT_dDP $(LT_DP_User = 0);
238  IR_DP = IR_DP_User $(LT_DP_User <> 0) + IR_dDP $(LT_DP_User = 0);
239
240  CRF_DP $(IR_DP + 1) = (IR_DP * (IR_DP + 1)**LT_DP) / ((IR_DP + 1)**LT_DP - 1);
241
242  CAP_DP(sc,time) = sum(time_ $ time_.first, CAP_DP(sc,time_)) $(Ind_CostDyn = 0) + CAP_DP(sc,time) $(Ind_CostDyn = 1);
243
244  */// DAC Plant Cost
245  Cost_DP_CC02(sc,time) = (CAP_DP(sc,time) * CRF_DP + OM_DP(sc));
246  Cost_DP_SC02(sc,time) = Cost_DP_CC02(sc,time) * CC02_DACCS(sc) / SC02_DACCS(sc);
247  Cost_DP_RC02(sc,c,time) = Cost_DP_CC02(sc,time) * CC02_DACCS(sc) / RC02_DACCS(sc,c,time);
248
249  CAPEX_CC02(sc,time) = CAP_DP(sc,time) * CRF_DP;
250  CAPEX_SC02(sc,time) = CAPEX_CC02(sc,time) * CC02_DACCS(sc) / SC02_DACCS(sc);
251  CAPEX_RC02(sc,c,time) = CAPEX_CC02(sc,time) * CC02_DACCS(sc) / RC02_DACCS(sc,c,time);
252
253  OPEX_CC02(sc) = OM_DP(sc);
254  OPEX_SC02(sc) = OPEX_CC02(sc) * CC02_DACCS(sc) / SC02_DACCS(sc);
255  OPEX_RC02(sc,c,time) = OPEX_CC02(sc) * CC02_DACCS(sc) / RC02_DACCS(sc,c,time);
256
257  *// CO2 Transport & Storage Cost
258
259  */// Financial Parameters
260  CRF_CO2T $(IR_CO2T + 1) = (IR_CO2T * (IR_CO2T+1) **LT_CO2T) / ((IR_CO2T + 1)** LT_CO2T - 1);
261
262  */// CO2 Transport Cost
263  Cost_CO2T_CC02 = (CAP_CO2T * D_CO2T * CRF_CO2T) /Capa_CO2T + OP_CO2T;
264  Cost_CO2T_SC02(sc) = (CAP_CO2T * D_CO2T * CRF_CO2T + OP_CO2T * Capa_CO2T) /Capa_CO2T * CC02_DACCS(sc) / SC02_DACCS(sc);
265  Cost_CO2T_RC02(sc,c,time) = (CAP_CO2T * D_CO2T * CRF_CO2T + OP_CO2T * Capa_CO2T) /Capa_CO2T * CC02_DACCS(sc) / RC02_DACCS(sc,c,time);

```

Figure 16: Economic evaluation of DACCS based on all the costs incurred along its value chain.

The total costs of solid sorbent DACCS archetype has been reported as \$1,200/t CO₂ removed on Climeworks official website⁴¹. In contrast to the liquid solvent DACCS system, the solid sorbent DAC plant is a modular process that is operated in two time-steps, requiring more maintenance. For this process, we assume that the levelised CAPEX and the OPEX each account for an equal share of the cost of CO₂ capture (Figure 16).

3.4 Enhanced Weathering (EW)

This subsection presents the key assumptions and model parameterisation used to characterise enhanced weathering (EW) in the model prototype. EW is the process by which CO₂ is sequestered from the atmosphere through the dissolution of silicate minerals on the land surface. In this process, basic rocks are crushed and ground to small particles, and spread onto croplands or agricultural lands for permanent CDR. The model is refactored into several sub-models as shown in Figure 17.

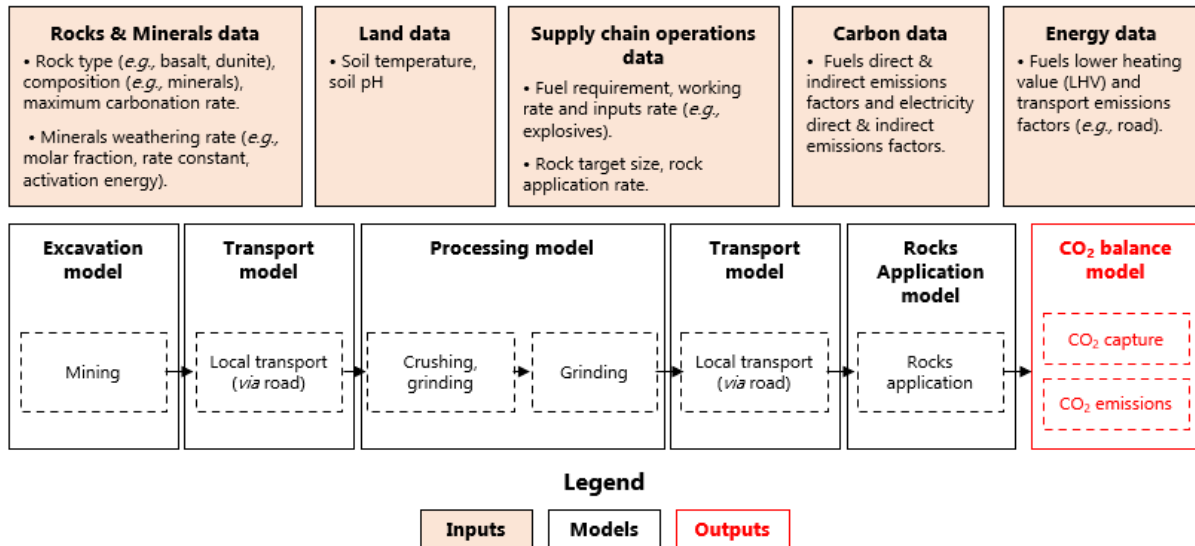


Figure 17: Schematic of the EW supply chain, outlining the interactions between the sub-models used in the model prototype.

In EW, rocks are excavated and transported to the grinding facility where they are crushed. The ground rock is transported to the area of application and spread on soil. The overall GHG emissions and economic performance of the technology is measured by the aggregate performance of the individual steps along the supply chain. Renforth⁴⁷ estimates the overall CDR potential of basic and ultrabasic rocks as 0.3 tonne CO₂/tonne rock and 0.8 tonne CO₂/tonne rock, respectively. Thus, greater quantities of basic rock are needed to store an equivalent amount of CO₂ compared to ultrabasic rocks, and in both cases, greater quantities of rock are needed relative to CO₂, increasing the requirement to excavate rocks and process them at scale.

We applied the exponential correlation developed by Strefler et al.⁴⁸ to estimate the energy required to grind the rock, given grain particle size distributions. Following which, the transport distance from the grinding facility to agricultural land is used together with the transported volumes to calculate the fuel requirements, and corresponding CO₂ emissions, assuming diesel fleets in the near-term. Note that the transport medium is a function of time as the ongoing decarbonisation of the transport sector will gradually reduce the overall CO₂ footprint associated with transport stage. The model has the capacity to use multiple fuels and zero-emission transport fleets to reflect the reductions in CO₂ intensity over time. The model incorporates region-specific data on soil temperature and pH to calculate the weathering rate.

The CO₂ sequestration potential of EW increases over time, as basic rocks weather, and saturates (permanently) over time. By then, the rocks have reached their maximum CO₂ sequestration potential, which is inherently rock-specific. The CDR potential of EW is a function of the technical potential of the rock, the carbonation to CO₂ sequestration conversion, and the rate of carbonation over time. The share of the rock that weathers every year is a function of the soil temperature⁴⁹, pH⁵⁰, mineral composition, and the size of rock⁸⁷. The rock weathering

rate is modelled using generalized equations as in (Beerling et al, 2020)⁵² and (Taylor et al, 2016)⁵³ and the carbonation rate is modelled with a shrinking core model, as suggested in (Renforth, 2012)⁴⁷.

The model prototype considers basalt, which is a basic rock, and dunite, which is an ultrabasic rock proposed in literature for EW applications. The overall GHG balance of EW in both cases are captured through the equations in Figure 18.

```

167  */ Carbon Balance
168  CF_M_RCO2(sr,sr_,r,p,p_,t,time) $(Ind_FeasibleOptTPort(sr,sr_,r,p,p_,t) AND tRCO2(sr,sr_,r,p,p_,t,time) < 0) = CF_M(sr,sr_,r,t,time) / tRCO2(sr,sr_,r,p,p_,t,time) * 1000;
169  CF_N2O_RCO2(sr,sr_,r,p,p_,t,time) $(Ind_FeasibleOptTPort(sr,sr_,r,p,p_,t) AND tRCO2(sr,sr_,r,p,p_,t,time) < 0) = CF_N2O(sr,sr_,r,t) / tRCO2(sr,sr_,r,p,p_,t,time) * 1000;
170  CF_R_RCO2(sr,sr_,r,p,p_,t,time) $(Ind_FeasibleOptTPort(sr,sr_,r,p,p_,t) AND tRCO2(sr,sr_,r,p,p_,t,time) < 0) = CF_R(sr,sr_,r,t,time) / tRCO2(sr,sr_,r,p,p_,t,time) * 1000;
171  CF_C_RCO2(sr,sr_,r,p,p_,t,time) $(Ind_FeasibleOptTPort(sr,sr_,r,p,p_,t) AND tRCO2(sr,sr_,r,p,p_,t,time) < 0) = CF_C(sr,sr_,r,t,time) / tRCO2(sr,sr_,r,p,p_,t,time);
172  CF_G_RCO2(sr,sr_,r,p,p_,t,time) $(Ind_FeasibleOptTPort(sr,sr_,r,p,p_,t) AND tRCO2(sr,sr_,r,p,p_,t,time) < 0) = CF_G(sr,sr_,r,t,time) / tRCO2(sr,sr_,r,p,p_,t,time) * 1000;
173  CF_T_RCO2(sr,sr_,r,p,p_,t,time) $(Ind_FeasibleOptTPort(sr,sr_,r,p,p_,t) AND tRCO2(sr,sr_,r,p,p_,t,time) < 0) = CF_T(sr,sr_,r,p,p_,t,time) / tRCO2(sr,sr_,r,p,p_,t,time);
174  CF_S_RCO2(sr,sr_,r,p,p_,t,time) $(Ind_FeasibleOptTPort(sr,sr_,r,p,p_,t) AND tRCO2(sr,sr_,r,p,p_,t,time) < 0) = CF_S(sr,sr_,r,t,time) / tRCO2(sr,sr_,r,p,p_,t,time) * 1000;
175  tCF_RCO2(sr,sr_,r,p,p_,t,time) $(Ind_FeasibleOptTPort(sr,sr_,r,p,p_,t) AND tRCO2(sr,sr_,r,p,p_,t,time) < 0) = tCF(sr,sr_,r,p,p_,t,time) / tRCO2(sr,sr_,r,p,p_,t,time) * 1000;
176  tCaCO2_RCO2(sr,sr_,r,p,p_,t,time) $(Ind_FeasibleOptTPort(sr,sr_,r,p,p_,t) AND tRCO2(sr,sr_,r,p,p_,t,time) < 0) = tCaCO2(sr,r) / tRCO2(sr,sr_,r,p,p_,t,time) * 1000;
177  tCCO2_RCO2(sr,sr_,r,p,p_,t,time) $(Ind_FeasibleOptTPort(sr,sr_,r,p,p_,t) AND tRCO2(sr,sr_,r,p,p_,t,time) < 0) = tCCO2(sr,r) / tRCO2(sr,sr_,r,p,p_,t,time) * 1000;
178
179
180  */ Key Output
181  Ind_maxNegScenario_EW(sr,sr_,r,p,p_,t,time) $(Ind_FeasibleOptTPort(sr,sr_,r,p,p_,t) AND tmaxRCO2(sr,sr_,r,p,p_,t,time) > 0) = yes;
182  Ind_NegScenario_EH(sr,sr_,r,p,p_,t,time) $(Ind_FeasibleOptTPort(sr,sr_,r,p,p_,t) AND tRCO2(sr,sr_,r,p,p_,t,time) > 0) = yes;

```

Figure 18: Equations which compute the CO₂ footprint of the various processes along the EW supply chain.

Similarly, the total costs of EW are parameterised using the following components:

- the CAPEX and OPEX of the mining and grinding facility, together with the cost of materials.
- the cost of diesel for mining rocks, transport, and application on soil, and electricity^{19–23} for crushing and grinding rocks.
- the cost of trucks to transport rocks, and tractors to apply them on soil.
- labour costs of digger, facility operator, and farmer.

Overall, the techno-economic parameters related to the individual technologies are represented using a consistent framework to compute various KPIs.

4. Summary of the optimisation model constraints

The optimisation framework combines the equations presented in section 3 with inequality constraints to define a pathway for NETP deployment across member states in Europe along with the United Kingdom. These inequality constraints are based on user inputs and assumptions on CDR deployment targets, and biogeophysical constraints. Given input data related to the individual technologies and regions as captured by NEGEM Deliverables 4.1 and 4.2, and member-state specific CDR targets as discussed in Deliverable 4.3, the mathematical model can determine pathways which minimise the: cost of CDR delivery, land use footprint, water footprint, primary energy demand, etc.

Burden-sharing principles were used in Deliverable 4.3 to generate a set of members-state specific CDR targets depending on global CDR requirements by 2100. The 4 scenarios proposed in Deliverable 4.3 are intended to be used in the modelling work within task 4.5. They allow the model to explore the cost, and environmental implications of different levels of CDR being “owned” by EU-28. The scenarios from Deliverable 4.3, together with different global CDR targets, combine to generate results with policy relevance on the value of different technologies. It is important to note that the application of burden-sharing principles via these scenarios leads to diverging shares of effort by the EU Member States, allowing a wide range of circumstances to be explored.

The targets are combined with deployment rate constraints specific to each technology. For BECCS, the availability of bioenergy is a rate limiting constraint. For DACCS, the market for the sorbents used in DACCS is likely to be the rate-limiting constraint as reported in the literature. We assume that BECCS and DACCS projects have a lifetime of 30 years. Following previous work, they are assumed to operate at base load⁵⁴⁻⁵⁷. We also assume that EW projects (*i.e.*, mining facility) have a lifetime of 20 years. Conversely, AR projects need to be maintained in perpetuity to avoid any reversal of CO₂ emissions back to the atmosphere.

Afforestation is limited by the availability of lands with a potential for reforestation (LPR), as defined in Griscom *et al.*⁵⁸. LPR are non-forested lands in areas ecologically suitable for forests with a low tree cover (< 25%) but within the boundaries of a native forest land type. Griscom *et al.*⁵⁸ exclude all land types categorised as grassland or savanna from LPR to limit negative impacts on biodiversity, cropland to account for food security, and land within boreal ecological zones to account for albedo effect.

Biomass for BECCS and biochar includes dedicated-energy crops cultivated on marginal agricultural lands (MAL), as defined in Cai *et al.*⁵⁹ and forestry residues and pellets. Following previous work⁶⁰, MAL is characterised here by mixed crop and natural vegetation land with marginal productivity. Therefore, the production of biomass for BECCS has no negative impacts on the agricultural sector and its associated food supply. The potential to exacerbate water stress must be minimised, and the model prototype limits the deployment of AR or the cultivation of biomass for BECCS to lands with low water stress, *i.e.* areas wherein the overall water risk is less than or equal to 3 on a 5-point scale, as defined in Gassert *et al.*⁶¹.

The global lithological map (GLiM) published by Hartmann and Moosdorf⁶² is used to constrain the availability of basalt and dunite in a given region. We assume a rock density of 2.9 t/m³^{347,53,63} and an extraction depth of 50m⁴⁷. Sub-regional geological CO₂ storage capacity is used here to constrain the deployment of geological CDR options such as BECCS and DACCS. This data is available at the national scale for the EU⁶⁴⁻⁶⁶.

Overall, the technology and region-specific constraints documented in Figure 19 provide the model with the capacity to generate deployment pathways that avoid an overreliance on any single CDR technology. This prototype version is undergoing further development prior to parameterisation and release as part of task 4.5.

```

439  */ BC Cost Equations
440
441  */ BC Non-Levelized Cost Equations
442  optcost_bc(Cfset_BC) $(sameAs(metric,'cost') AND Ind_lcost = 0) ..      Opt_Cost_BC(Cfset_BC) =e= Opt_LU_App_BC(Cfset_BC) * cost_BC(Cfset_BC);
443
444  cumutotalcost_bc(tc) $(sameAs(metric,'cost') AND Ind_lcost = 0) ..      CCost_BC(tc) =e= sum((pyp,sr,b,1,tc_) $(Cfset_BC(pyp,sr,b,1,tc_) AND ord(tc_) <= ord(tc)), Opt_
445
446  */ BC Levelized Cost Equations
447  optlcost_bc(Cfset_BC) $(sameAs(metric,'cost') AND Ind_lcost) ..          Opt_LCost_BC(Cfset_BC) =e= Opt_LU_App_BC(Cfset_BC) * cost_BC(Cfset_BC);
448
449  cumutotalcostb(tc) $(sameAs(metric,'cost') AND Ind_lcost) ..            CLCost_BC(tc) =e= sum((pyp,sr,b,1,tc_) $(Cfset_BC(pyp,sr,b,1,tc_) AND ord(tc_) <= ord(tc)), Opt
450
451  */ BC Cost Balance Equations
452
453  */ BC Non-Levelized Cost Balance Equations
454  optcostb_bc(Cfset_BC) $(sameAs(metric,'costB') AND Ind_lcost = 0) ..     Opt_CostB_BC(Cfset_BC) =e= Opt_LU_App_BC(Cfset_BC) * CB_BC(Cfset_BC);
455
456  cumutotalcostb_bc(tc) $(sameAs(metric,'costB') AND Ind_lcost = 0) ..     CCostB_BC(tc) =e= sum((pyp,sr,b,1,tc_) $(Cfset_BC(pyp,sr,b,1,tc_) AND ord(tc_) <= ord(tc)), Opt
457
458  */ BC Levelized Cost Balance Equations
459  optlcostb_bc(Cfset_BC) $(sameAs(metric,'costB') AND Ind_lcost) ..        Opt_LCostB_BC(Cfset_BC) =e= Opt_LU_App_BC(Cfset_BC) * CB_BC(Cfset_BC);
460
461  cumutotalcostb_bc(tc) $(sameAs(metric,'costB') AND Ind_lcost) ..        CLCostB_BC(tc) =e= sum((pyp,sr,b,1,tc_) $(Cfset_BC(pyp,sr,b,1,tc_) AND ord(tc_) <= ord(tc)), Op
462
463  */ BC Land Use Equations
464  optlusc_bc(Cfset_BC) ..                                                  Opt_LU_SC_BC(Cfset_BC) =e= Opt_LU_App_BC(Cfset_BC) * LU_SC_BC(Cfset_BC);
465
466  optlup_bc(Cfset_BC) $ sameAs(metric,'land')..                          Opt_LU_P_BC(Cfset_BC) =e= Opt_LU_App_BC(Cfset_BC) * LU_P_BC(Cfset_BC);
467
468  totallu_bc(tc) $ sameAs(metric,'land') ..                               tLU_BC(tc) =e= sum((pyp,sr,b,1) $(Cfset_BC(pyp,sr,b,1,tc)), Opt_LU_SC_BC(pyp,sr,b,1,tc) + Opt_L
469
470  */ BC Water Use Equations
471  optmwu_bc(Cfset_BC) $ sameAs(metric,'water')..                        Opt_MWU_BC(Cfset_BC) =e= MWU_BC(Cfset_BC) * Opt_LU_App_BC(Cfset_BC);
472
473  cumutotalmwu_bc(tc) $ sameAs(metric,'water') ..                       CMWU_BC(tc) =e= sum((pyp,sr,b,1,tc_) $(Cfset_BC(pyp,sr,b,1,tc_) AND ord(tc_) <= ord(tc)), Opt_M
474
475  */ BC Biomass Use Equations
476  optbu_bc(Cfset_BC) $ Ind_Syn ..                                         Opt_BU_BC(Cfset_BC) =e= BU_BC(Cfset_BC) * Opt_LU_App_BC(Cfset_BC);
477  totalc_bu_bc(c,b,1,tc) $ Ind_Syn ..                                     c_BU_BC(c,b,1,tc) =e= sum((pyp,sr) $(Cfset_BC(pyp,sr,b,1,tc) AND Ind_Country(sr,c)), Opt_BU_BC(

```

Figure 19: Equality and inequality constraints in the optimisation formulation to provide bounds for the key decision variable – the amount of each CDR technology to deploy to meet the cumulative CDR target across member states in the EU.

To prepare this report, the following deliverable has been taken into consideration:

D#	Deliverable title	Lead Beneficiary	Type	Dissemination level	Due date (in MM)
D 1.1	Justification of NETPs chosen for the NEGEM project	ETH	Report	CO	6
D 1.4	Comprehensive sustainability assessment of Bio-CCS NETPs	VTT	Report	PU	12
D 1.5	Comprehensive sustainability assessment of geoengineering and other NETPs	ICL	Report	PU	24
D 4.1	NETP database	ICL	Database	PU	4
D 4.2	Bio-geophysics database	ICL	Database	PU	12
D 4.3	Member State targets	ICL	Report	PU	15
D 8.1	Stocktaking of scenarios with negative emission technologies and practises	VTT	Report	PU	8

5. References

1. Hurteau, M. D., Hungate, B. A. & Koch, G. W. Accounting for risk in valuing forest carbon offsets. *Carbon Balance Manag.* **4**, 1 (2009).
2. Whittaker, C., Mortimer, N., Murphy, R. & Matthews, R. Energy and greenhouse gas balance of the use of forest residues for bioenergy production in the UK. *Biomass and Bioenergy* **35**, 4581–4594 (2011).
3. Whittaker, C. L., Mortimer, N. D. & Matthews, R. W. *Understanding the carbon footprint of timber transport in the United Kingdom. North Energy, report* (2010).
4. Morison, J. *et al. Understanding the carbon and greenhouse gas balance of forests in Britain.* (2012).
5. Aldentun, Y. Life cycle inventory of forest seedling production — from seed to regeneration site. *J. Clean. Prod.* **10**, 47–55 (2002).
6. Timmermann, V. & Dibdiakova, J. Greenhouse gas emissions from forestry in East Norway. *Int. J. Life*

- Cycle Assess.* **19**, 1593–1606 (2014).
7. Berg, S. & Karjalainen, T. Comparison of greenhouse gas emissions from forest operations in Finland and Sweden. *Forestry* **76**, 271–284 (2003).
 8. Kenney, J., Gallagher, T., Smidt, M., Mitchell, D. & McDonald, T. Factors that Affect Fuel Consumption in Logging Systems. in *37th Council on Forest Engineering Annual Meeting* (2014).
 9. Röder, M., Whittaker, C. & Thornley, P. How certain are greenhouse gas reductions from bioenergy? Life cycle assessment and uncertainty analysis of wood pellet-to-electricity supply chains from forest residues. *Biomass and Bioenergy* **79**, 50–63 (2015).
 10. BEIS. *MS Excel Spreadsheet - Greenhouse gas reporting - conversion factors 2020: full set (for advanced users)*. (2020).
 11. Camargo, G. G. T., Ryan, M. R. & Richard, T. L. Energy use and greenhouse gas emissions from crop production using the farm energy analysis tool. *Bioscience* **63**, 263–273 (2013).
 12. Lewandowski, I., Kicherer, A. & Vonier, P. CO₂-balance for the cultivation and combustion of *Miscanthus*. *Biomass and Bioenergy* **8**, 81–90 (1995).
 13. Elsayed, M. A., Matthews, R. & Mortimer, N. D. *Carbon and energy balances for a range of biofuels options*. DTI Sustainable Energy Programs (2003).
 14. De Klein, C. *et al.* Chapter 11 : N₂O emissions from managed soils. in *Volume 4: Agriculture, Forestry and Other Land Use - IPCC Guidelines for National Greenhouse Gas Inventories* 1–54 (2006).
 15. Parajuli, R. *et al.* Life Cycle Assessment of district heat production in a straw fired CHP plant. *Biomass and Bioenergy* **68**, 115–134 (2014).
 16. Murphy, F., Devlin, G. & McDonnell, K. *Miscanthus* production and processing in Ireland: An analysis of energy requirements and environmental impacts. *Renew. Sustain. Energy Rev.* **23**, 412–420 (2013).
 17. Mekonnen, M. M. & Hoekstra, A. Y. The green, blue and grey water footprint of crops and derived crop products. *Hydrol. Earth Syst. Sci.* **15**, 1577–1600 (2011).
 18. World Bank. Pump price for diesel fuel (US\$ per liter). (2020).
 19. Ministry of Mines and Energy. *Monthly Energy Bulletin - December 2018*. (2018).
 20. CEIC. Price of electricity. (2020).
 21. EUROSTAT. Electricity prices by type of user (EUR per kWh). (2020).
 22. Government of India. *Evaluation Report on Rajiv Gandhi Grameen Vidyutikaran Yojana*. (2014).
 23. Energy Information Administration. Average retail price of electricity (cents per kilowatthour). (2020).
 24. Brinker, R. W., Kinard, J., Rummer, R. & Lanford, B. *Machine rates for selected forest harvesting machines*. (2002).
 25. Johansson, J., Liss, J.-E., Gullberg, T. & Björheden, R. Transport and handling of forest energy bundles—advantages and problems. *Biomass and Bioenergy* **30**, 334–341 (2006).
 26. US Bureau of Labor Statistics. Occupational Employment and Wage Statistics. (2019).
 27. Duffy, M. *Estimated Costs for Production, Storage and Transportation of Switchgrass*. *Biomass and Bioenergy* (2008).
 28. de Wit, M. & Faaij, A. European biomass resource potential and costs. *Biomass and Bioenergy* **34**, 188–

- 202 (2010).
29. ALBA TREES. ALBA TREES - The UK's largest producer of cell grown plants. (2020).
 30. HomeGuide. How Much Does Crushed Stone or Gravel Cost? (2020).
 31. World Bank. Official exchange rate (LCU per US\$, period average). (2020).
 32. World Bank. inflation, GDP deflator (annual%). (2020).
 33. Fargione, J., Hill, J., Tilman, D., Polasky, S. & Hawthorne, P. Land Clearing and the Biofuel Carbon Debt. *Science (80-.)*. **319**, 1235–1238 (2008).
 34. Plevin, R. J., O'Hare, M., Jones, A. D., Torn, M. S. & Gibbs, H. K. Greenhouse gas emissions from biofuels' indirect land use change are uncertain but may be much greater than previously estimated. *Environ. Sci. Technol.* **44**, 8015–8021 (2010).
 35. Overmars, K. P., Stehfest, E., Ros, J. P. M. & Prins, A. G. Indirect land use change emissions related to EU biofuel consumption: An analysis based on historical data. *Environ. Sci. Policy* **14**, 248–257 (2011).
 36. Fajardy, M. & Mac Dowell, N. Can BECCS deliver sustainable and resource efficient negative emissions? *Energy Environ. Sci.* **10**, 1389–1426 (2017).
 37. Fajardy, M. Developing a framework for the optimal deployment of negative emissions technologies. (Imperial College London, 2020).
 38. International Energy Agency. *World Energy Outlook 2016*. (2016).
 39. National Academies of Sciences Engineering and Medicine. *Negative Emissions Technologies and Reliable Sequestration: A Research Agenda*. (2019) doi:10.17226/25259.
 40. Keith, D. W., Holmes, G., St. Angelo, D. & Heidel, K. A Process for Capturing CO₂ from the Atmosphere. *Joule* 1–22 (2018) doi:10.1016/j.joule.2018.05.006.
 41. Climeworks. Climeworks. (2020).
 42. Hu, A. & Dong, Q. On natural gas pricing reform in China. *Nat. Gas Ind. B* **2**, 374–382 (2015).
 43. EUROSTAT. Gas prices by type of user (EUR per gigajoule). (2020).
 44. Energy Information Administration. Natural Gas Prices (Dollards per Thousandf Cubic Feet). (2020).
 45. Sanz-Pérez, E. S., Murdock, C. R., Didas, S. A. & Jones, C. W. Direct Capture of CO₂ from Ambient Air. *Chem. Rev.* **116**, 11840–11876 (2016).
 46. Fuss, S. *et al.* Negative emissions - Part 2: Costs, potentials and side effects. *Environ. Res. Lett.* **13**, (2018).
 47. Renforth, P. The potential of enhanced weathering in the UK. *Int. J. Greenh. Gas Control* **10**, 229–243 (2012).
 48. Strefler, J., Amann, T., Bauer, N., Kriegler, E. & Hartmann, J. Potential and costs of carbon dioxide removal by enhanced weathering of rocks. *Environ. Res. Lett.* **13**, (2018).
 49. Wan, Z., Hook, S. & Hulley, G. MOD11C3 MODIS/Terra Land Surface Temperature/Emissivity Monthly L3 Global 0.05Deg CMG V006. (2015) doi:https://doi.org/10.5067/MODIS/MOD11C3.006.
 50. Wieder, W. R., Boehnert, J., Bonan, G. B. & Langseth, M. RegridDED Harmonized World Soil Database

v1.2. (2014) doi:10.3334/ORNLDAAC/1247.

51. Rinder, T. & von Hagke, C. The influence of particle size on the potential of enhanced basalt weathering for carbon dioxide removal - Insights from a regional assessment. *J. Clean. Prod.* **315**, 128178 (2021).
52. Beerling, D. J. *et al.* Potential for large-scale CO₂ removal via enhanced rock weathering with croplands. *Nature* **583**, 242–248 (2020).
53. Taylor, L. L. *et al.* Enhanced weathering strategies for stabilizing climate and averting ocean acidification. *Nat. Clim. Chang.* **6**, 402–406 (2016).
54. Daggash, H. A. & Mac Dowell, N. The implications of delivering the UK's Paris Agreement commitments on the power sector. *Int. J. Greenh. Gas Control* **85**, 174–181 (2019).
55. Daggash, H. A. & Mac Dowell, N. Structural Evolution of the UK Electricity System in a below 2°C World. *Joule* **3**, 1239–1251 (2019).
56. Daggash, H. A., Heuberger, C. F. & Mac Dowell, N. The role and value of negative emissions technologies in decarbonising the UK energy system. *Int. J. Greenh. Gas Control* **81**, 181–198 (2019).
57. Daggash, H. A. & Mac Dowell, N. Higher Carbon Prices on Emissions Alone Will Not Deliver the Paris Agreement. *Joule* **3**, 2120–2133 (2019).
58. Griscom, B. W. *et al.* Natural climate solutions. *Proc. Natl. Acad. Sci. U. S. A.* **114**, 11645–11650 (2017).
59. Cai, X., Zhang, X. & Wang, D. Land Availability for Biofuel Production. *Environ. Sci. Technol.* **45**, 334–339 (2011).
60. Fajardy, M., Chiquier, S. & Mac Dowell, N. Investigating the BECCS resource nexus: delivering sustainable negative emissions. *Energy Environ. Sci.* **11**, 3408–3430 (2018).
61. GASSERT, F., LANDIS, M., LUCK, M., REIG, P. & SHIAO, T. *AQUEDUCT GLOBAL MAPS 2.1*. (2015).
62. Hartmann, J. & Moosdorf, N. The new global lithological map database GLiM: A representation of rock properties at the Earth surface. *Geochemistry, Geophys. Geosystems* **13**, (2012).
63. Beerling, D. J. *et al.* Farming with crops and rocks to address global climate, food and soil security. *Nat. Plants* **4**, 138–147 (2018).
64. Vangkilde-Pedersen, T. *et al.* Assessing European capacity for geological storage of carbon dioxide – the EU GeoCapacity project. *Energy Procedia* **1**, 2663–2670 (2009).
65. Poulsen, N., Holloway, S., Neele, F., Smith, N. A. & Kirk, K. CO₂StoP Final Report Assessment of CO₂ storage potential in Europe. (2011).
66. Gammer, D. *A Picture of CO₂ Storage in the UK - Learnings from ETI's UKSAP and derived Projects*. (2015).